Partitioning of Large and Minichromosomes in Trypanosoma brucei

Klaus Ersfeld, *et al.*

Science **276**, 611 (1997);
DOI: 10.1126/science.276.5312.611

Science (print ISSN 0036-8075; online ISSN 1095-9203) is published weekly, except the last week in December, by the American Association for the Advancement of Science, 1200 New York Avenue NW, Washington, DC 20005.

11889 (1994).
16. J. P. Duguid and D. C. Old, in *Bacterial Adherence, Receptors and Recognition*, E. H. Beachey, Ed. (Chapman & Hall, London, 1977), pp. 184–217; J. E. Salit and E. Gotschlich, *J. Exp. Med*. **146**, 1182 (1977); I. Ofek, A. Mosek, N. Sharon, *Infect. Immun*. **34**, 708 (1981); A. J. Schaeffer, S. K. Amundsen, L. N. Schnidt, *ibid.* **24**, 753 (1979).
17. S. J. Hultgren, T. N. Porter, A. J. Schaeffer, J. L. Duncan, *Infect. Immun*. **50**, 370 (1985).
18. S. J. Hultgren, W. R. Schwann, A. J. Schaeffer, J. L. Duncan, *ibid.* **54**, 613 (1986).
19. H. L. T. Mobley *et al*., *Mol. Microbiol*. **10**, 143 (1993).
20. H. Connell *et al*., *Proc. Natl. Acad. Sci. U.S.A.* **93**, 9827 (1996).
21. L. Maurer and P. E. Orndorff, *J. Bacteriol*. **169**, 640 (1987); M. S. Hanson and C. C. Brinton, *ibid.* **170**, 3350 (1988); S. N. Abraham, J. D. Goguen, D. Sun, P. Klemm, E. H. Beachey, *ibid.* **169**, 5530 (1987).
22. P. Falk *et al*., *Proc. Natl. Acad. Sci. U.S.A*. **90**, 2035 (1993); D. R. Cundell, N. P. Gerard, C. Gerard, I. Idanpaan-Heikkila, E. I. Tuomanen, *Nature* **377**, 435 (1995); J. W. St. Geme III, *Infect. Immun.* **62**, 3881 (1994); R. Lindstedt *et al*., *ibid.* **57**, 3389 (1989).
23. To assess mannose inhibition of binding activity by type 1–piliated NU14, we suspended fluorescein isothiocyanate (FITC)–labeled NU14 in a 15% mannose solution in phosphate-buffered saline (PBS) before the in situ tissue hybridization assay described in Fig. 1.
24. A suicide vector, pJEB521, was constructed by insertion of a fragment containing the type 1 operon region (with a chloramphenicol resistance marker inserted into the *fimH* gene at the Kpn I site) into the pCVD442 suicide plasmid {provided by M. Lombardo, M. S. Donenberg, and J. B. Kaper [*Infect. Immun*. **59**, 4310 (1991)]}. PCR analysis of the pJEB521 plasmid confirmed correct insertion of the chloramphenicol resistance marker in the *fimH* gene. The *fimH*$^-$ strain, NU14-1, was constructed by introducing pJEB521 from SM10λpir into the *E. coli* clinical isolate NU14 by filter mating. Selection for incorporation of the *fimH* knockout sequences into the NU14 strain was by chloramphenicol and ampicillin resistance, with subsequent analysis for the loss of the ability to hemagglutinate guinea pig red blood cells. Colonies that had lost hemagglutination activity were repeatedly passed in liquid media lacking ampicillin. Serial dilutions were plated on chloramphenicol media and screened for the loss of ampicillin resistance, indicative of the loss of suicide vector sequences. Chloramphenicol-resistant colonies that were ampicillin sensitive were again screened for the inability to hemagglutinate guinea pig red blood cells. One such colony (ampicillin sensitive, chloramphenicol resistant, hemagglutination negative) was designated NU14-1 and used for the binding studies as well as for further comparative studies; DNA blots of chromosomal DNA from NU14-1 confirmed that the mutation was specifically at the *fim*H locus. Electron microscopy revealed that the mutation also greatly reduced piliation.
25. P. E. Orndorff and S. Falkow, *J. Bacteriol*. **159**, 736 (1984); F. Jacob-Dubuisson, F. Heuser, K. Dodson, S. Normark, S. J. Hultgren, *EMBO J*. **12**, 837 (1993).
26. F. C. Minion, S. N. Abraham, E. H. Beachey, J. D. Goguen, *J. Bacteriol*. **165**, 1033 (1989).
27. New Zealand White rabbits (female, 2.5 kg) were injected subcutaneously with 200 μg of FimC-H, FimHt, or whole type 1 pili (day 0) and boosted with 50 μg of each of the corresponding proteins (week 4). Bleeds were obtained every 3 to 4 weeks, and endpoint titers to FimH and whole type 1 pili were determined by enzyme-linked immunosorbent assay (ELISA) as described in Fig. 2.
28. H. Li and D. H. Walker, *Infect. Immun*. **60**, 2030 (1992).
29. W. W. Agace *et al.*, *ibid.* **61**, 602 (1993).
30. *Escherichia coli* was isolated from urine specimens obtained from adult female or pediatric patients with urinary tract infections at Columbia Presbyterian Medical Center in New York or Children's Hospital in Boston, MA. Bacteria were grown in static broth at 37°C for 48 hours to induce type 1 pilus expression (*24*). Expression of type 1 pili was confirmed by hemagglutination of a 3% solution of guinea pig erythrocytes and inhibition of hemagglutination by a 10 mM solution of α-methyl mannoside (*39*).
31. D. C. Dodd and B. I. Eisenstein, *Infect. Immun*. **38**, 764 (1982).
32. *Escherichia coli* strains were induced for P pilus expression by overnight growth on tryptic soy agar (TSA) at 37°C. Organisms were tested for mannose-resistant hemagglutination (MRHA) of a 3% suspension of human red blood cells (HuRBCs) to screen for P pilus expression. Strains that were positive for MRHA of 3% HuRBCs were tested for inhibition by antisera to PapGII to confirm P pilus expression. *Escherichia coli* strains were also tested for MRHA of a 3% suspension of swine red blood cells (SwRBCs) to screen for S pilus expression.
33. L. Hagberg *et al*., *Infect. Immun*. **40**, 273 (1983); P. O'Hanley, D. Lark, S. Falkow, G. Schoolnik, *J. Clin. Invest*. **75**, 347 (1985); H. L. T. Mobley *et al*., *Infect. Immun*. **58**, 1281 (1990).
34. Two groups of C3H/HeJ mice were inoculated on day 0 and boosted at week 4 with purified FimHt protein (15 μg in CFA, then in IFA, respectively) or with CFA or IFA adjuvant alone and challenged with 5 × 10^7 CFU of type 1–piliated *E. coli* strain NU14 at week 29 after immunization. The average number of colony-forming units per bladder for each group of 10 mice was evaluated as described for Fig. 4C 2 days after the intraurethral challenge. A 100-fold reduction was seen in the number of recoverable organisms for FimHt-immunized mice as compared with CFA or IFA naïve controls ($P = 0.0001$).
35. H. H. Collins *et al.*, *J. Infect. Dis*. **159**, 1073 (1989); S. M. Opal *et al*., *ibid.* **161**, 1148 (1990).
36. X. R. Wu, T. T. Sun, J. J. Medina, *Proc. Natl. Acad. Sci. U.S.A.* **93**, 9630 (1996).
37. M. M. Levine, R. E. Black, C. C. Brinton, *Scand. J. Infect. Dis. Suppl*. **33**, 83 (1982).
38. S. Marieke van Ham, L. van Alphen, F. R. Mooi, J. P. M. van Putten, *Infect. Immun*. **63**, 4883 (1995); K. W. McCrea, W. J. Watson, J. R. Gilsdorf, C. F. Marrs, *ibid.* **62**, 4992 (1994); B. Lund, F. P. Lindberg, M. Baga, S. Normark, *J. Bacteriol*. **162**, 1293 (1985); M. J. Kuehn, J. Heuser, S. Normark, S. J. Hultgren, *Nature* **356**, 252 (1992); X. Nassif *et al*., *Proc. Natl. Acad. Sci. U.S.A.* **91**, 3769 (1994); T. Rudel, I. Scheuerpflug, T. F. Meyer, *Nature* **373**, 357 (1995).
39. R. Striker, U. Nilsson, A. Stonecipher, G. Magnusson, S. J. Hultgren, *Mol. Microbiol*. **16**, 1021 (1995).
40. J. P. Duguid, S. Clegg, M. I. Wilson, *J. Med. Microbiol*. **12**, 213 (1979); N. Firon, I. Ofek, N. Sharon, *Carbohydr. Res*. **120**, 235 (1983); C. S. Giampapa, S. N. Abraham, T. M. Chiang, E. H. Beachey, *J. Biol. Chem*. **263**, 5362 (1988).
41. The bacteria–epithelial cell mixtures in the binding assay were incubated while being mixed at 37°C to achieve maximal binding, then gently washed two times with PBS to remove nonadherent bacteria; after the second wash the epithelial cell pellet was resuspended in PBS, and the samples were assayed by flow cytometry. Background fluorescence was determined by analysis of J82 cells alone.
42. Mice were inoculated with bacteria by inserting a polyethylene catheter adapted to a flat-end 30-gauge needle on a 1-ml tuberculin syringe into the bladder transurethrally and infusing 0.05 ml of a bacterial suspension in PBS. Two days after challenge, the mice were killed and the bladders were removed aseptically, homogenized, and cultured on TSA plates supplemented with streptomycin. To assess ascending infection into the kidney, we killed the mice and removed the kidneys aseptically 7 days after challenge, homogenized them, and cultured them on TSA plates supplemented with streptomycin.
43. Supported by NIH grant RO1DK51406 and by MedImmune (S.J.H.). S.J.H. and Washington University have a financial interest in MedImmune.

20 August 1996; accepted 14 March 1997

Partitioning of Large and Minichromosomes in *Trypanosoma brucei*

Klaus Ersfeld* and Keith Gull

The *Trypanosoma brucei* nuclear genome contains about 100 minichromosomes of between 50 to 150 kilobases and about 20 chromosomes of 0.2 to 6 megabase pairs. Minichromosomes contain nontranscribed copies of variant surface glycoprotein (VSG) genes and are thought to expand the VSG gene pool. Varying VSG expression allows the parasite to avoid elimination by the host immune system. The mechanism of inheritance of *T. brucei* chromosomes was investigated by in situ hybridization in combination with immunofluorescence. The minichromosome population segregated with precision, by association with the central intranuclear mitotic spindle. However, their positional dynamics differed from that of the large chromosomes, which were partitioned by kinetochore microtubules.

Trypanosoma brucei is a flagellated protozoan parasite that separated from the eukaryotic lineage very early in the evolution of eukaryotes (*1*, *2*). The extracellular parasite survives in the bloodstream of the host by periodically changing its VSG coat, a process known as antigenic variation (*3*). VSG genes, which are the only known open reading frames on the 100 or so minichromosomes of *T. brucei*, are transcriptionally inactive (*4*–*8*). Minichromosomes are thought to increase the repertoire of VSG genes, which can be transposed to expression sites on the larger chromosomes (*9*).

In eukaryotic cells, chromosomes are typically segregated by association with a bipolar mitotic spindle. This ensures an almost perfect mechanism to faithfully segregate chromosomes during cell division. Although there is an intranuclear mitotic spindle in *T. brucei*, indirect evidence argues against a microtubule-dependent segregation mechanism for at least part of the genome. Elec-

University of Manchester, School of Biological Sciences, 2.205 Stopford Building, Oxford Road, Manchester M13 9PT, UK.

*To whom correspondence should be addressed. E-mail: klaus.ersfeld@man.ac.uk

tron microscopic (EM) studies of dividing *T. brucei* nuclei indicate that the mitotic spindle contains insufficient microtubules to provide a conventional centromere-microtubule interaction for all of the more than 100 chromosomes (*2*, *10*). Rather, the chromatin of dividing *T. brucei* cells seems to be closely associated with the nuclear envelope (*10*, *11*). In a more recent study, in situ hybridization was used to demonstrate a peripheral localization of minichromosomes in the nucleus of interphase cells of trypanosomes (*12*).

Given genetic evidence of mitotic stability (*13*) yet uncertainty over the segregation mechanism, we addressed the question of where chromosomes of procyclic *T. brucei* are located during the cell cycle and how their segregation is achieved. To visualize spindle microtubules, we used a monoclonal antibody (KMX) specific for β-tubulin (*14*, *15*). Fluorescence in situ hybridization (FISH) was used to visualize DNA segments of individual chromosomes (*16*, *17*). To locate minichromosomes, we used a 177–base pair (bp) repeat sequence (MC177) as a probe (*18*). This sequence is specific for minichromosomes and has been used previously to study their distribution in interphase cells (*12*). To visualize a DNA segment on one of the larger chromosomes, we chose the 5*S* ribosomal DNA (R5S) because this gene exists as a linear array of hundreds of tandem repeats on one of the chromosomes larger than 4 megabase pairs (Mbp) (*19*, *20*). The segregation pattern observed for the chromosome carrying the 5*S* genes is likely to be representative of the large chromosomes of *T. brucei* in general. In support of this hypothesis, very similar results were obtained with genomic DNA clones covering about 150 kilobase pairs of the tubulin locus located in the center of a chromosome of about 1 Mbp (*21*). The small size of even the largest chromosomes of *T. brucei* and the size and position of the target DNA sequences used for FISH exclude trailing effects of those loci in relation to potential centromeres, which have not yet been identified.

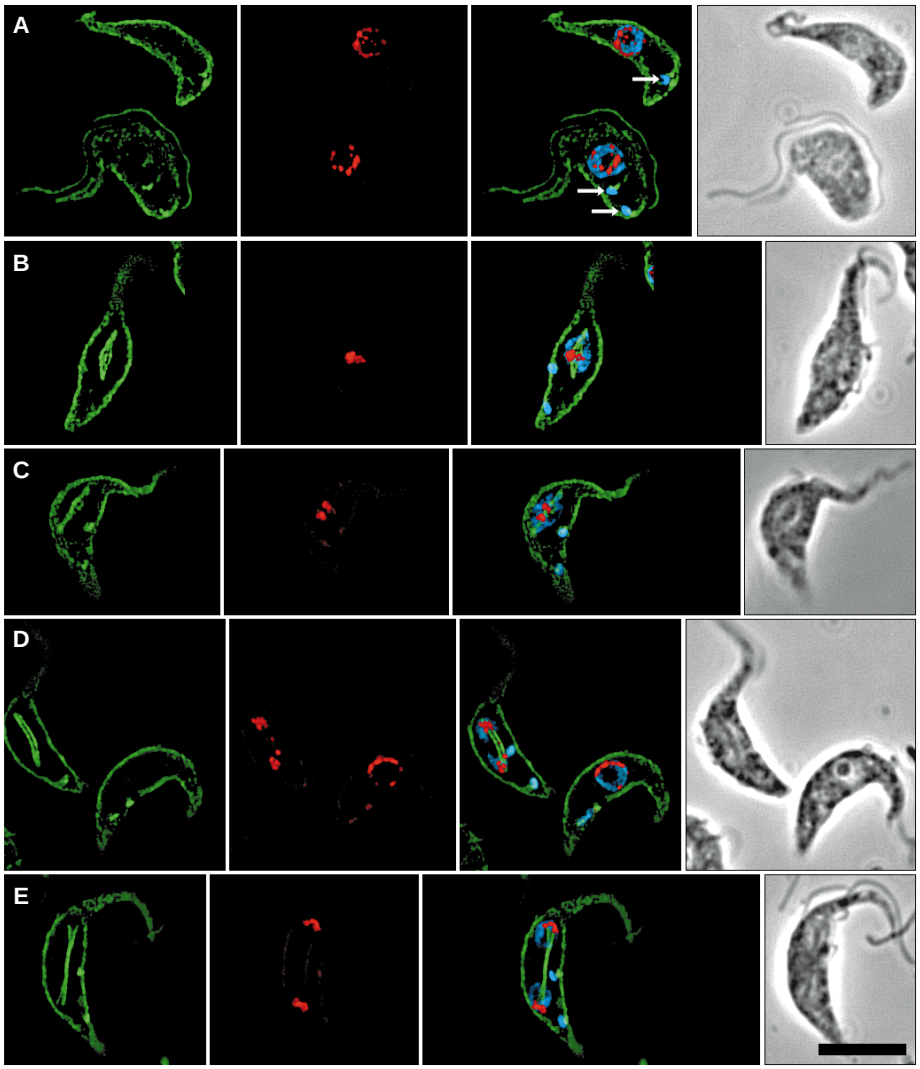

Fig. 1. The distribution of minichromosomes during the cell division cycle. (**A**) In interphase, minichromosomes were asymmetrically distributed near the nuclear periphery (see also right cell in D). (**B**) After formation of a spindle, minichromosomes congregated in the nuclear center. (**C** to **E**) During progression of mitosis, the minichromosomes separated into two entities and relocated to the poles of the spindle. The minichromosomal signal is shown in red, the antibody to tubulin in green, and the total DNA in blue. The third and fourth frame of each row represent the merged signals and the phase-contrast image, respectively. The kinetoplasts as markers for cell cycle progression are labeled by arrows (first row only). Bar, 10 μm.

Although chromosomes in trypanosomes do not visibly condense, probably as a result of their unusual histone composition (*22*), it is relatively easy to follow the progression of mitosis using nuclear elongation and segregation of the mitochondrial kinetoplast as markers (*10*, *23*). Elongation of the nucleus indicates the onset of mitosis. The nucleolus does not disperse during mitosis but elongates and acquires a dumbbell shape before it splits into two entities preceding karyokinesis.

During interphase the minichromosomes were located in small clusters distributed asymmetrically around the periphery of the nucleus (Fig. 1, A and D). As the cells progressed toward M phase, a reorganization occurred. During the transition from G_2 to M phase, the small minichromosome groups started to aggregate into larger and fewer clusters. Once the cell had clearly entered mitosis, indicated by the appearance of a small spindle, the minichromosomes congressed into one mass in the center of the nucleus (Fig. 1B). The mitotic spindle of trypanosomes consists of a central array of densely packed microtubules plus peripheral microtubules; the latter might represent pole-to-kinetochore microtubules because they terminate in electron-dense structures resembling the kinetochores described in higher eukaryotes (*10*, *11*). After the establishment of the spindle, the minichromosomal DNA split into two equal-sized clusters that subsequently moved to the poles of the spindle (Fig. 1, C and D). As the central spindle elongated, the minichromosomes remained at their polar position (Fig. 1E). Late in mitosis the poles of the spindle were close to the nuclear envelope with the minichromosomes still attached. After the disassembly of the spindle, shortly before nuclear division, the minichromosomes congregated close to the nuclear envelope. This distribution pattern could still be observed in cells during and after cytokinesis; only later, during S and G_2 phases, did the clusters disintegrate into smaller units (Fig. 1A, lower cell). This explained the nonrandom spatial

distribution of minichromosomes in G_1 cells and, to a lesser extent, in S phase (*12*).

The segregation of large chromosomes, as deduced by the 5S ribosomal gene cluster localization, followed a different pattern (Figs. 2 and 3). Based on the analysis of many cells, the two dots representing the G_1-phase diploid and, after S phase, the tetraploid chromosome complement did not exhibit a preferential localization within the nucleus (Fig. 2A). After DNA replication the R5S signals were still visible as two single dots because the sister chromosomes had not yet segregated (Fig. 2B). In early mitosis, when the minichromosomes were still congregated in the center of the nucleus, the R5S signals occupied a position near the nuclear periphery (Fig. 2B). Once the minichromosomes were positioned at the spindle poles, the R5S signals trailed behind and relatively closer to the midpoint of the spindle (Fig. 2C), suggesting different velocities of polar movement. As mitosis progressed, the R5S dots were frequently found at the outer periphery of the central spindle (Figs. 2, C and D, and 3, A and B), consistent with the position of kinetochore-like structures in spindles of dividing nuclei at these stages seen in EM images (*11*, *24*). In late anaphase the R5S dots eventually moved closer to the poles but never overlapped with the minichromosomal locations (Figs. 2D and 3C).

To demonstrate the dependence of minichromosomal segregation on an intact mitotic spindle, we treated trypanosomes with the drug rhizoxin, which disassembles microtubules (*25*). A concentration of 5 to 20 nM rhizoxin affects the integrity of the spindle but leaves other microtubule-containing structures, such as the subpellicular cytoskeleton and the axoneme of the flagellum, largely unaffected. Treatment of cells for 4 hours with 5 nM rhizoxin resulted in the formation of aberrant spindle morphology in mitotic cells (Fig. 4A). Minichromosomes in these cells still associated with the malformed spindles but failed to segregate to the poles. Instead, they often formed rod-shaped structures along bundles of microtubules. After treatment with 10 nM rhizoxin for 4 hours a spindle was no longer visible, but in some cells small tubulin-containing structures could be detected at a position corresponding to the poles of the former spindle (Fig. 4B). Treatment with 20 nM rhizoxin prevented any reorganization of minichromosomes in cells that, according to the position of their kinetoplasts, should have entered mitosis (Fig. 4C).

We propose the following model for the mechanism of chromosome segregation in *T. brucei*. Minichromosomes congregate in the center of the nucleus at the onset of mitosis. This aggregation may, or may not,

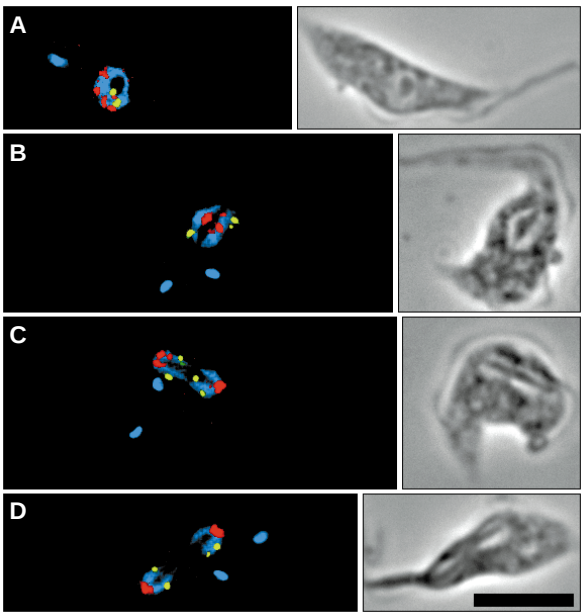

Fig. 2. Minichromosomes (red) and large chromosomes (yellow) exhibit different positional dynamics during mitosis. (**A**) During interphase the R5S signal was located in a central position within the nucleus, whereas minichromosomes were close to the nuclear envelope. (**B**) On the onset of mitosis minichromosomes congregated in the center of the nucleus, whereas the 5S signals were near the periphery of the nucleus. (**C** and **D**) As mitosis progressed, minichromosomes became localized at the spindle poles and the 5S dots were closer to the center of the spindle. The approximate position of the spindle corresponds to the black exclusion zone between the DNA (blue) and by the dark structure inside the nucleus in the corresponding phase-contrast images, which is caused by the spindle and the persistent nucleolus. Bar, 10 μm.

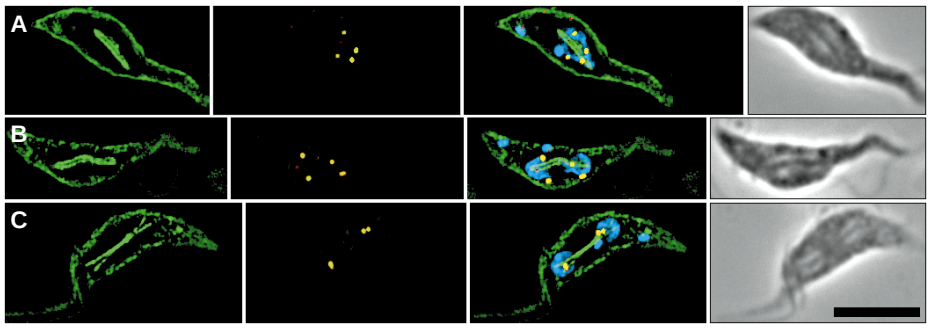

Fig. 3. The localization of a large chromosome during mitosis. (**A** and **B**) In early stages of anaphase the 5S ribosomal gene signal (yellow) was located outside the central spindle (green). (**C**) In late anaphase, shortly before karyokinesis, the dots were much closer to the spindle poles. Phase-contrast images are shown on the far right. Bar, 10 μm.

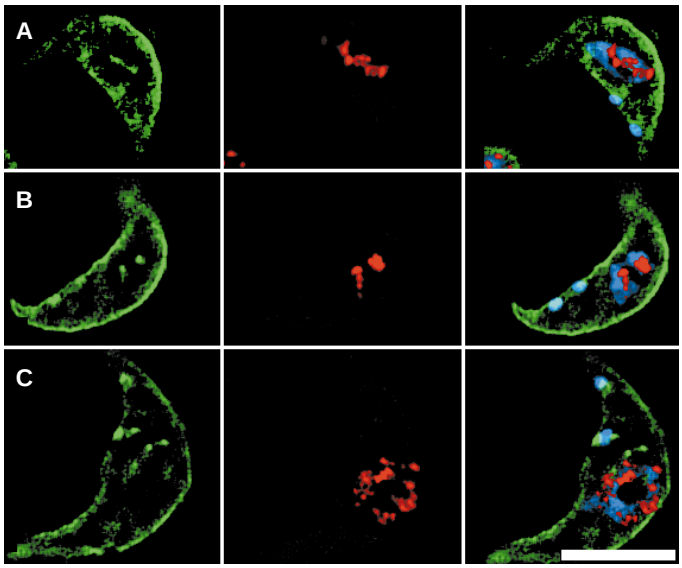

Fig. 4. The effect of the anti-microtubule drug rhizoxin on the segregation of minichromosomes (color designation as in Fig. 1). (**A**) Rhizoxin (5 nM) still allowed a small spindle to form but prevented the polar organization of minichromosomes; they remained distributed alongside the entire spindle. (**B**) At 10 nM the drug prevented spindle formation but left two small structures. Minichromosomes colocalized with these structures, which were interpreted as spindle pole remnants. (**C**) Rhizoxin (20 nM) inhibited spindle formation completely and prevented minichromosomes from reorganizing in the nuclear center at the onset of mitosis. The interkinetoplast distance (the two DAPI-stained dots) indicated that the cell should have entered mitosis by this time. Bar, 10 μm.

be preceded by a condensation of the chromosomes. After association with the emerging central spindle, they separate into two clusters that move to opposite spindle poles. They remain at the spindle poles during spindle elongation until they are in close proximity to the nuclear envelope. Their asymmetrical distribution within the nucleus is maintained after spindle disassembly until late S phase when they are distributed almost randomly near the nuclear envelope. As the ploidy is uncertain and individual minichromosomes cannot be visualized owing to the lack of large enough specific target DNA sequences, it is not clear whether there is faithful segregation of each minichromosome. However, detailed microscopic analysis of many cells (>100) showed that the minichromosomal clusters segregated on the spindle and inherited by each daughter cell were of equivalent size, indicating a precise segregation mechanism.

The existence of a highly coordinated segregation mechanism for minichromosomes suggests that they play an important role in the biology of this parasite. In addition, owing to their small size, minichromosomes may serve as an excellent model for the study of mitotic segregation, particularly with respect to the evolution of DNA partition mechanisms. The diploid large chromosomes, as exemplified by the chromosome harboring the 5*S* ribosomal gene, are likely segregated by peripheral pole-to-kinetochore microtubules. There is, however, an intriguing discrepancy between the number of large chromosomes, estimated to be at least 20 for the diploid set (*4*, *21*), and the number of kinetochore-like structures, estimated to be approximately 10 (*11*, *24*).

REFERENCES AND NOTES

1. L. Sogin, *Curr. Opin. Genet. Dev.* **1**, 453 (1991).
2. K. Vickerman, *Int. J. Parasitol.* **24**, 1317 (1994).
3. G. A. M. Cross, *BioEssays* **18**, 283 (1996).
4. K. Gottesdiener, J. Garcia-Anoveros, M. G. Lee, L. H. T. van der Ploeg, *Mol. Cell. Biol.* **10**, 6079 (1990).
5. L. H. T. van der Ploeg, D. C. Schwartz, C. R. Cantor, P. Borst, *Cell* **37**, 77 (1984).
6. P. Sloof *et al*., *J. Mol. Biol.* **167**, 1 (1983).
7. M. Weiden, Y. N. Osheim, A. L. Beyer, L. H. T. van der Ploeg, *Mol. Cell. Biol.* **11**, 3823 (1991).
8. R. O. Williams, J. R. Young, P. A. O. Majiwa, *Nature* **299**, 417 (1982).
9. L. H. T. van der Ploeg, A. W. C. A. Cornelissen, J. D. Barry, P. Borst, *EMBO J.* **3**, 3109 (1984).
10. K. Vickerman and T. M. Preston, *J. Cell Sci.* **6**, 365 (1970).
11. A. J. Solari, *Biocell* **19**, 65 (1995).
12. H. M. M. Chung, C. Shea, S. Fields, R. N. Taub, L. H. T. van der Ploeg, *EMBO J.* **9**, 2611 (1990).
13. J. C. B. M. Zomerdijk, R. Kieft, P. Borst, *Nucleic Acids Res.* **20**, 2725 (1992).
14. R. Sasse and K. Gull, *J. Cell Sci.* **90**, 577 (1988).
15. C. R. Birkett, K. E. Foster, L. Johnson, K. Gull, *FEBS Lett.* **187**, 211 (1985).
16. For combined immunofluorescence and fluorescence in situ hybridization, procyclic trypanosomes (strain 427) were washed once in phosphate-buffered saline (PBS), transferred to slides coated with aminopropyltriethoxysilane (Sigma), and fixed with 4% formaldehyde–5% acetic acid in PBS for 15 min at 20°C. After washing twice with PBS, cells were permeabilized with 0.1% NP-40 in PBS for 5 min, washed once in PBS, and incubated with the first antibody in PBS for 1 hour, then washed three times for 5 min each in PBS and incubated with a secondary, fluorescein isothiocyanate (FITC)–conjugated antibody (Dako) for 45 min. After washing, cells were postfixed in 3% formaldehyde for 20 min. Cells were then prehybridized for 60 min in 50% formamide, 2× saline sodium phosphate–EDTA (SSPE), 10% dextran sulfate [hybridization buffer (HB)] at 37°C, and subsequently hybridized as described in (*17*).
17. For in situ hybridization, digoxigenin- or biotin-labeled DNA probes were coprecipitated with herring sperm DNA (10 mg/ml) and yeast tRNA (10 mg/ml), respectively, and resuspended in HB. After prehybridization, probes in HB were transferred to the slide, sealed with a plastic frame (Geneframe, Hybaid, Teddington, UK), and denatured simultaneously with the cellular DNA on an in situ block (Hybaid) at 95°C for 5 min and hybridized at 37°C for 16 hours. Washing was done in 50% formamide, 2× standard saline citrate (SSC) for 30 min at 37°C, 10 min in 2× SSC at 50°C, 60 min in 0.2× SSC at 50°C, and 10 min in 4× SSC at 20°C. For detection of digoxigenin-labeled probes, cells were then incubated with a sheep anti-digoxigenin Fab fragment (Boehringer Mannheim) in 100 mM maleic acid, 150 mM NaCl, 1% blocking reagent (Boehringer) (MEB) for 1 hour at 20°C, washed in tris-buffered saline plus 0.1% Tween-20, and incubated with an FITC-conjugated antibody to sheep immunoglobulin G (Jackson Laboratory) for 45 min in MEB. For detection of biotinylated DNA, cells were incubated with a streptavidin-CY3 conjugate (Sigma) for 1 hour at 20°C in MEB. After washing as above, cells were mounted in Vectashield (Vector Laboratories) containing 4′,6′-diamidino-2-phenylindole (DAPI; 0.1 μg/ml). Cells were analyzed on a Leitz DMRB microscope, and images were captured by means of a slow-scan cooled charge-coupled device camera (Photometrics) and IPLab software (Sigma Analytics). Images were deconvoluted with HazeBuster software (VayTek) and pseudocolored and merged in Adobe Photoshop on a Macintosh 9500/132 computer.
18. The minichromosomal 177-bp repeat element was amplified by polymerase chain reaction (PCR) with the primers (5′-GCGAATTCTAAATGGTTCTTATACGAATG) and (5′-TACGAAGCTTAACACTAAAGAACAGCGTTG) (*6*, *7*). The ribosomal 5*S* DNA was amplified with the primers (5′-GCGAATTCAATCTATGCCAATC) and (5′-TACGAAGCTTCTGATCGCCGTACTAACGAG) (*20*). Purified PCR products were labeled by PCR with either digoxigenin (ribosomal probe) or biotin (minichromosomal probe) with the same sets of primers and a 1:2 ratio of digoxigenin or biotin-dUTP and dTTP. Labeled PCR products were purified on Qiagen spin columns.
19. G. Hasan, M. J. Turner, J. S. Cordingley, *Gene* **27**, 75 (1984).
20. J. S. Cordingley, *Mol. Biochem. Parasitol.* **17**, 321 (1985).
21. S. Melville, personal communication.
22. M. Burri *et al*., *Biol. Cell* **83**, 23 (1995).
23. T. Sherwin and K. Gull, *Philos. Trans. R. Soc. London Ser. B* **323**, 573 (1989).
24. I. Alieva, I. Vorobjev, E. Ogbadoyi, K. Ersfeld, K. Gull, unpublished results; K. Ersfeld and K. Gull, unpublished results.
25. D. R. Robinson, T. Sherwin, A. Ploubidou, E. H. Byard, K. Gull, *J. Cell Biol.* **128**, 1163 (1995).

26. We thank members of our lab for discussion. DNA probes of the tubulin locus were obtained from S. Melville, University of Cambridge. The work in our lab was supported by a Wellcome Trust Programme and Equipment Grant. K.E. is supported by a Wellcome Trust Postdoctoral Fellowship.

1 November 1996; accepted 25 February 1997

Continuous in Vitro Evolution of Catalytic Function

Martin C. Wright and Gerald F. Joyce*

A population of RNA molecules that catalyze the template-directed ligation of RNA substrates was made to evolve in a continuous manner in the test tube. A simple serial transfer procedure was used to achieve approximately 300 successive rounds of catalysis and selective amplification in 52 hours. During this time, the population size was maintained against an overall dilution of 3×10^{298}. Both the catalytic rate and amplification rate of the RNAs improved substantially as a consequence of mutations that accumulated during the evolution process. Continuous in vitro evolution makes it possible to maintain laboratory "cultures" of catalytic molecules that can be perpetuated indefinitely.

The principle of Darwinian evolution is applicable in vitro when a population of informational macromolecules is subjected to repeated rounds of selective amplification and mutation. An earlier extracellular Darwinian evolution experiment was done with variants of Qβ bacteriophage genomic RNA that were amplified on the basis of their ability to serve as a substrate for the Qβ replicase protein (*1*). Evolution was made to occur in a continuous manner by serial transfer of the RNAs to successive reaction vessels. In recent years, in vitro evolution procedures have been generalized to encompass almost any nucleic acid molecule, including those that have catalytic function (*2*). Unlike the Qβ evolution experiments, however, the evolution of catalytic function has been carried out in a stepwise rather than continuous fashion. Stepwise evolution requires intervention by

Departments of Chemistry and Molecular Biology and The Skaggs Institute for Chemical Biology, The Scripps Research Institute, 10550 North Torrey Pines Road, La Jolla, CA 92037, USA.

*To whom correspondence should be addressed.